Optik 122 (2011) 919–923

Contents lists available at ScienceDirect

Optik

journal homepage: www.elsevier.de/ijleo

Measurement of surface resistivity/conductivity of metallic alloys in aqueous solutions by optical interferometry techniques

K. Habib*

Materials Science Lab., Department of Advanced Systems, KISR, P.O. Box 24885 SAFAT, 13109 Kuwait

ARTICLE INFO

Article history:
Received 13 November 2009
Accepted 9 June 2010

Keywords:
Electrical resistivity
Electrical conductivity
Electrical resistance
Holographic interferometry
Metallic alloys

ABSTRACT

Optical interferometry techniques were used for the first time to measure the surface resistivity/conductivity of the pure aluminium (in seawater at room temperature), UNS No.304 stainless steel (in seawater at room temperature), and pure copper (in tap water at room temperature) without any physical contact. This was achieved by applying an electrical potential across the alloys and measuring the current density flow across the alloys, during the cyclic polarization test of the alloys in different solutions. In the mean time, optical interferometry techniques such as holographic interferometry were used in situ to measure the orthogonal surface displacement of the alloys, as a result of the applied electrical potential. In addition, a mathematical model was derived in order to correlate the ratio of the electrical potential to the current density flow (electrical potential/electronic current flow = resistance) and to the surface (orthogonal) displacement of the metallic samples. In other words, a proportionality constant (surface resistivity or conductivity = 1/surface resistivity) between the measured electrical resistance and the surface displacement (by the optical interferometry techniques) was obtained. Consequently the surface resistivity (ρ) and conductivity (σ) of the pure aluminium (in seawater at room temperature), UNS No.304 stainless steel (in seawater at room temperature), and pure copper (in tap water at room temperature) were obtained. Also, electrical resistivity values (ρ) from other source were used for comparison sake with the calculated values of this investigation. This study revealed that the measured value of the resistivity for the pure aluminium ($7.7 \times 10^{10}\,\Omega$ cm in seawater at room temperature) is in good agreement with the one found in literature for the aluminium oxide, 85% Al_2O_3 ($5 \times 10^{10}\,\Omega$ cm in air at temperature 30 °C). Unfortunately, there is no measured value for the resistivity of cupric oxide (CuO), cuprous oxide (Cu_2O), or even the oxide of the UNS No.304 stainless steel in literature comparing those values with the measured values in this study.

1. Introduction

In a previous work conducted by the author [1], a mathematical model was derived in order to relate the electrical resistance of the oxide film on a metal sample (surface) to the thickness of the oxide film on the metal sample. The mathematical model can be described as the following:

$$R = \frac{\rho U_{\text{total}}}{A} \tag{1}$$

where R is the electrical resistance of the oxide film (Ω). ρ is the electrical resistivity of the oxide film (Ω cm). A is surface area of the sample (cm^2). U_{total} is the total thickness of the oxide film which can be obtained by holographic interferometry, a non-contact technique (μm).

U_{total} can be determined as the following:

$$U_{\text{total}} = \frac{N\lambda}{\sin\alpha + \sin\beta} \tag{2}$$

where N is the number of fringes. λ is the wavelength of the laser light used in the experiment, for He–Ne laser light ($\lambda = 0.6234\,\mu$m). α is the illumination angle ($\alpha = 47.23°$). β is the viewing angle ($\beta = 90°$), both α and β can be obtained from the set up of the experiment.

A detailed derivation of Eqs. (1) and (2) is given elsewhere in literature [2,3].

Eq. (1) has been used to obtain the electrical resistance of aluminium oxide film, Al_2O_3, on pure aluminium samples in different concentrations of sulphuric acid solutions by using optical interferometry techniques [1].

Eq. (1) also can be used to measure the surface resistivity/conductivity of metallic alloys in aqueous solutions. This can be achieved by laser holographic interferometry in order to measure the total surface orthogonal displacement, U_{total}, during the

* Tel.: +965 795 6296; fax: +965 543 0239.
E-mail address: khaledhabib@usa.net.

0030-4026/$ – see front matter © 2010 Elsevier GmbH. All rights reserved.
doi:10.1016/j.ijleo.2010.06.018

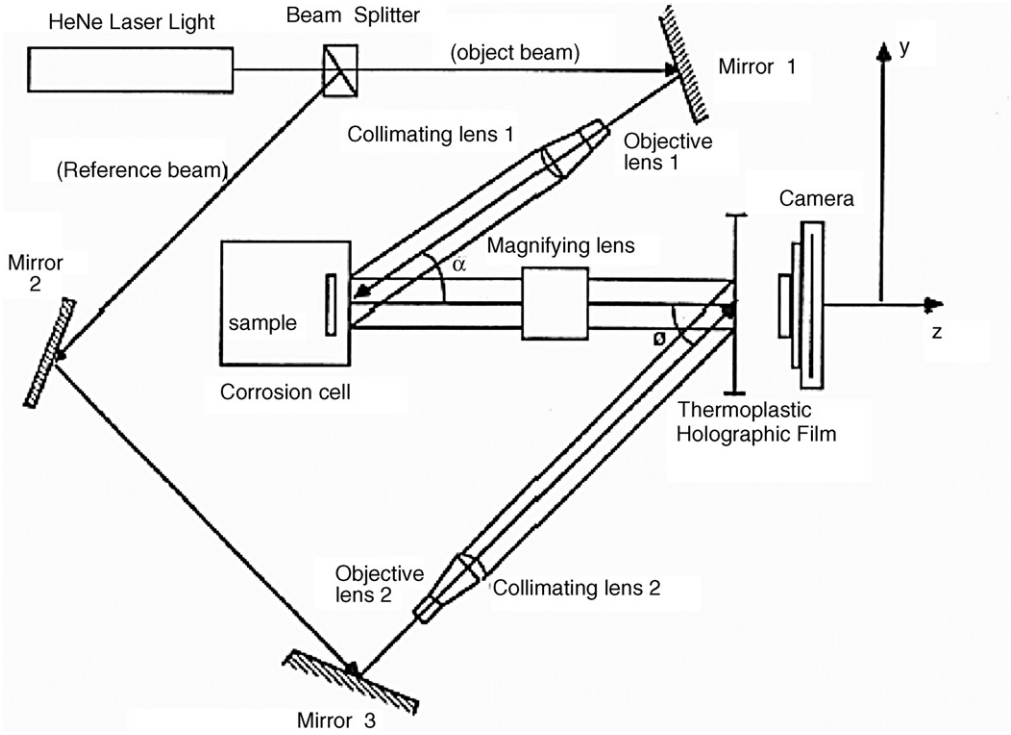

Fig. 1. Optical setup of an off axis holographic interferometry.

electrical polarization of the metallic alloys in the aqueous solutions, from Eq. (2). This implies that an electrical potential will be first applied on the metallic alloys. Then the produced current density flow across the metallic alloys, as the result of the electrical potential, will be measured. Eventually, a correlation can be developed, from Eq. (1), between the ratio of the applied electrical potential to the current density flow (electrical potential/current density flow = resistance × area) and to the surface (orthogonal) displacement (U_{total}) of the metallic alloys, from Eq. (2). In other words, a proportionality constant (surface resistivity = ρ or conductivity = $1/\rho = \sigma$) between the measured electrical resistance and the total surface displacement (by the optical interferometry techniques) can be obtained. Consequently the surface resistivity/conductivity of the metallic alloys can be determined, without any physical contact.

2. Experimental work

Metallic samples of pure aluminium (99.7% Al), UNS No.304 stainless steel (18–20% Cr, 8–11% Ni, 2%max Mn, 1%max Si, and 0.08%max C) and pure copper (99.8% Cu) were used in this investigation. The pure aluminium samples were fabricated in a cylindrical form with dimensions of 8 cm in diameter and 0.15 cm in thickness. The rest of the samples was fabricated in a rectangular form with dimensions of 10.0 cm × 10.0 cm × 0.15 cm for this investigation. Then all samples were polished and ground by silicon carbide papers until the finest grade (1200 grade) was reached. In order to be sure that the aluminium samples have attained scratch-free surface, the samples were etched by a chemical solution for 2 min at temperature ranged between 85 and 95 °C. The etching solution made of 3 g/L of sodium hydroxide + 30 g/L of tri-sodium phosphate. Then a coal tar (black) epoxy (polyamide cured) was used on one side and all edges of all samples. The reason for covering one side and all the edges of the samples by the coal tar epoxy is for protection from the solutions while testing the other side of the samples (side exposed to solution). At the beginning of each test, each sample was immersed in a particular solution for 1 h. While the sample was in the solution, the corrosion potential was monitored by a voltmeter with respect to a Saturated Calomel Electrode (SCE), reference electrode. After the sample attained steady state corrosion potential, a hologram of the sample was recorded using an off axis holography, see Figs. 1 and 2 for the optical set up. In the meantime cyclic polarization was conducted on the sample with the hologram recording of the sample in the solution. In this study, a camera with a thermoplastic film was used to facilitate recordings of the holographic interferograms of the samples. The camera is HC-300 Thermoplastic Recorder made by Newport Corporation. Also, in this study, a potentialstat model 273 made by EG&G Princeton applied research was used to conduct the cyclic polarization test for determining the surface resistivity/conductivity of the three metallic alloys in different aqueous solutions. During each experiment, the holographic interferograms were recorded as a function of time, in which each test lasted for less than 60 min, the duration of cyclic polarization of the samples in solutions. Then, the interferograms were interpreted to an orthogonal displacement of the surface of the metal by using Eq. (2). Also, by knowing the applied potential for

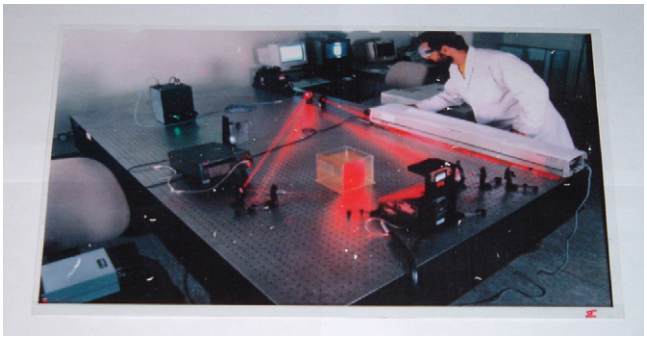

Fig. 2. A photograph image of the laboratory of the off axis holographic interferometry.

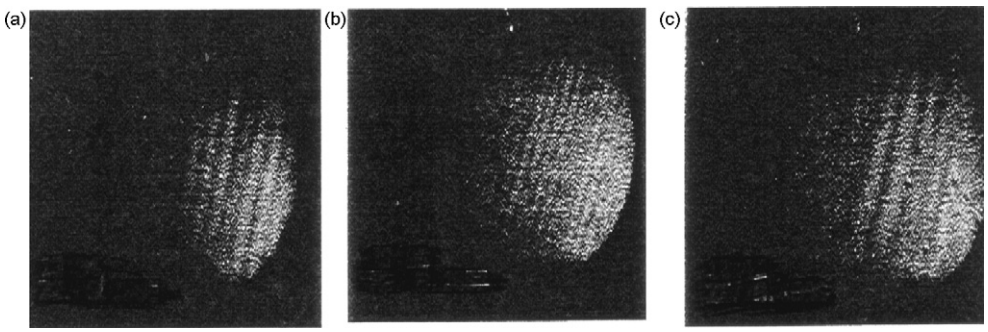

Fig. 3. Progressive interferogram of aluminium sample in seawater as a function of cyclic polarization: (a) at −350 mV vs. SCE (see Fig. 4); (b) at −300 mV vs. SCE; (c) at 100 mV vs. SCE.

each interferograms and the corresponding current density flow, from cyclic polarization plots, one can determine from the resistance (R) of the metallic alloys, from the slope of the linear portion of the cyclic polarization plots. It is worth mentioning that more than one recording of the real-time holographic interferograms of the samples was necessary in this investigation, because of the high density of the number of fringes which appeared during the cyclic polarization test of some of the metallic samples in solutions.

3. Results and discussion

Fig. 3a–c shows progressive interferograms of the pure aluminium sample in seawater as a function of cyclic potential. Fig. 3a represents a real-time interferogram of the sample during cyclic polarization (at −350 mV vs. SCE), where 11 fringes appeared on the photograph. This figure indicates that an oxide layer was uniformly formed on the aluminium sample during the forward cyclic polarization in the positive direction, see Fig. 4 for the cyclic polarization of aluminium in seawater. It is obvious from this photograph that there is a general chemical attack, i.e. anodization of the aluminium sample depicted by the uniform interferometric pattern. Fig. 3b is the same interferogram of the sample during cyclic polarization (at −300 mV vs. SCE, see Fig. 4), where 18 fringes are detected on the photograph. Fig. 3c is the same interferogram of the sample during cyclic polarization (at +100 mV vs. SCE, see Fig. 4), where 9 fringes are detected on the photograph. The decrease of the number of fringes was due to the formation of hydrogen bubbles on the sample surface at which the hydrogen overvoltage was reached just at the end of the forward cyclic polarization of the aluminium in seawater. It is clear from Fig. 3c that some bubbles still remained on the right side of the figure. From Fig. 3a–c, the U_{total} = 6.52 μm, was determined from Eq. (2).

Fig. 4 shows points (a–c) on the hysteresis loop indicating exactly from where the interferograms (Fig. 3a–c) were taken during the cyclic polarization test. From Fig. 4, the resistance, RA = $5 \times 10^7\ \Omega\,cm^2$, of the aluminium sample was determined from the slope of the linear portion between point a and c, see Fig. 5. Consequently, the resistivity, $\rho = 7.7 \times 10^{10}\ \Omega$ cm and the conductivity ($\sigma = 1.3 \times 10^{-11}$ S/cm) of the aluminium sample was determined from Eq. (1).

Fig. 6a–e shows progressive interferograms of UNS No.304 stainless steel sample in seawater as a function of time. Fig. 6a represents a real-time interferogram of the sample during cyclic polarization (at −0.32 V vs. SCE), where 6–7 fringes appeared on the photograph. This indicates that a general mass removal took place on a microscopic scale in the forward direction of the cathodic region of cyclic polarization of the stainless steel in seawater (Fig. 7). Because the mass removal took place on a microscopic scale, 1–2 μm in the cathodic region of the cyclic polarization, it most likely occurred due to a uniform desorption of materials on the surface of the stainless steel sample. This sort of surface phenomenon, i.e. surface adsorption and desorption, can be documented by holographic interferometry because of the high spatial resolution of the technique, 0.3 μm. Fig. 6b is the same interferogram of the sample during cyclic polarization (at −0.1 V vs. SCE, see Fig. 7), where 18–20 fringes were detected on the photograph. Fig. 6c is the same interferogram of the sample during cyclic polarization (at +0.22 V vs. SCE, see Fig. 7), where 32–34 fringes were detected on the photograph. Fig. 6a–c shows a progressive general attack, surface desorption and uniform corrosion from the cathodic region to the anodic region in the forward direction of the cyclic polarization of the stainless steel in seawater. Because of the high density of the number of fringes which clearly appeared in Fig. 8c, a new (second) holographic interferogram was recorded. Fig. 8d is the second interferogram of the

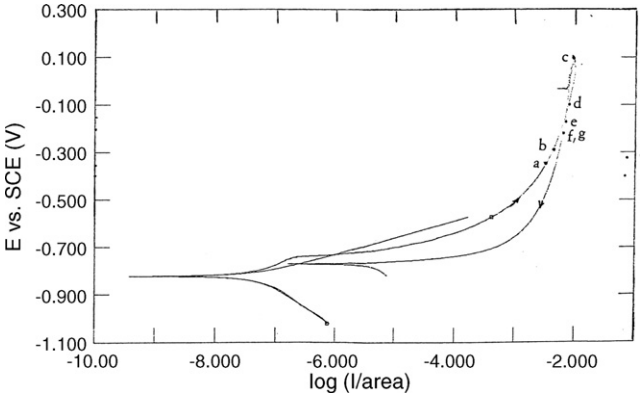

Fig. 4. The cyclic polarization plot of aluminium in seawater, which contains points (a–g) on the hysteresis loop indicating exactly from where the interferograms (Fig. 3a–c) were taken during the cyclic polarization test.

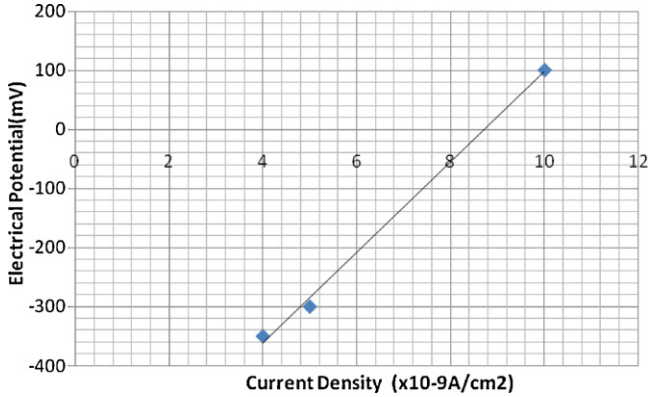

Fig. 5. shows a plot of the applied electrical potential vs. the corresponding current density, between points a and c in Fig. 4, of the pure aluminium sample in seawater.

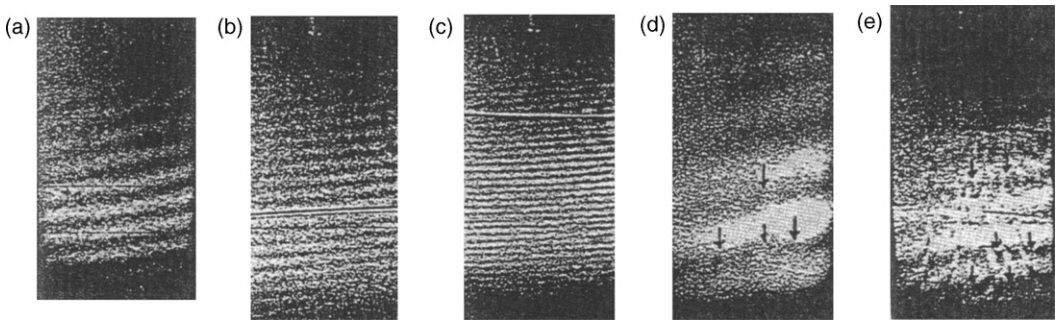

Fig. 6. Progressive interferogram of UNS No.304 stainless steel sample in seawater as a function of cyclic polarization: (a) at −0.32 V vs. SCE (see Fig. 7) in forward direction of cyclic polarization; (b) at −0.1 V vs. SCE; (c) at +0.22 V vs. SCE; (d) at +0.42 V vs. SCE; (e) at +0.5 V vs. SCE.

sample during cyclic polarization (at +0.42 V vs. SCE, see Fig. 7), where 4–5 fringes were detected on the photograph. It is obvious that in Fig. 6d there is localized, i.e. pitting corrosion, at a depth range between 0.3 μm and several micrometers, which appeared as localized perturbations in interferometric patterns at the bottom and middle portions on the interferograms (see arrows in Fig. 6d). The spacing between the fringes is no longer uniform at the bottom and middle portions of the interferogram (Fig. 6d), due to the localized attack. Fig. 6e is the same interferogram of the sample during cyclic polarization (at +0.5 V vs. SCE, see Fig. 7), where 7–8 fringes were detected on the photograph. It is obvious from this interferogram that the number as well as the depth of localized perturbation increased almost all over the sample. From Fig. 3a–c, the U_{total} = 6.52 μm, was determined from Eq. (2).

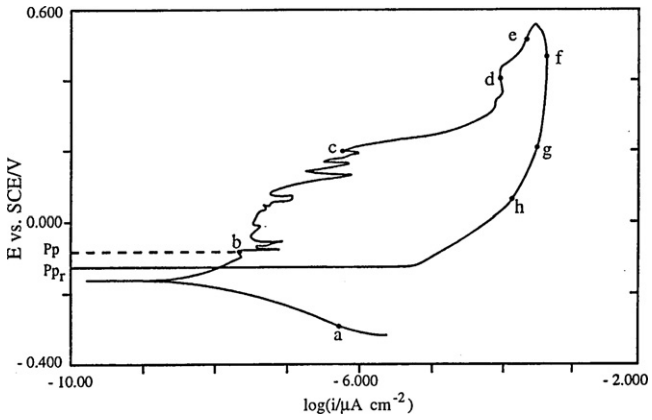

Fig. 7. The cyclic polarization of UNS No.304 stainless steel in seawater.

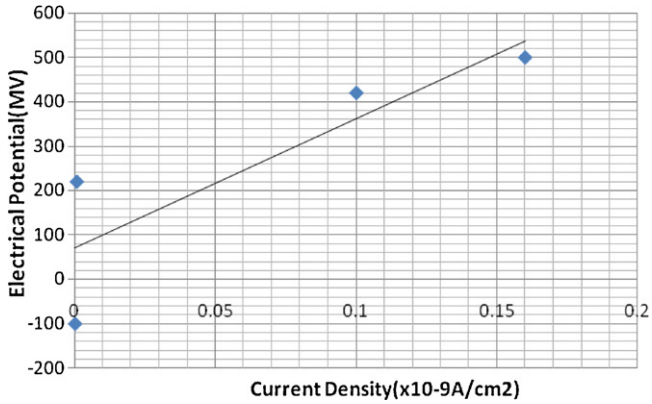

Fig. 8. A plot of the applied electrical potential vs. the corresponding current density, between points b and e in Fig. 7, of the UNS No.304 stainless steel sample in seawater.

Fig. 7 shows points (a–e) on the hysteresis loop indicating exactly from where the interferograms (Fig. 6a–e) were taken during the cyclic polarization test. From Fig. 7, the resistance, RA = 2.94 × 10^9 Ω cm^2, of the UNS No.304 stainless steel sample was determined from the slope of the linear portion between point b and e, see Fig. 8. Consequently, the resistivity, ρ = 2 × 10^{14} Ω cm and the conductivity (σ = 5 × 10^{-15} S/cm) of the UNS No.304 stainless steel sample was determined from Eq. (1).

Fig. 9 represents the cyclic polarization of copper in tap water. In the case of copper sample in tap water, fringes were observed only in the reverse direction of the cyclic polarization, see point a–c in Fig. 9. At point a (at +0.35 V vs. SCE) in Fig. 9, 3 fringes were detected in interferograms of Fig. 9, in a similar fashion of Figs. 3 and 6 for the aluminium and stainless steel samples, respectively. Furthermore, at point b (at +0.2 V vs. SCE), 6 fringes were detected in interferograms of Fig. 9. In contrast, a localized attack, pitting corrosion, was initially detected as interferometric perturbations, in the reverse direction of the cyclic polarization at point c (at +0.15 V vs. SCE), where 9 fringes were detected in interferograms of Fig. 9.

From the obtained data of Fig. 9, the U_{total} = 3.3 μm, was determined from Eq. (2).

Fig. 9 shows points (a–c) on the hysteresis loop indicating exactly from where interferograms were taken during the cyclic polarization test of the copper sample in tap water. From Fig. 10, the resistance, RA = 8.33 × 10^9 Ω cm^2, of the copper sample was determined from the slope of the linear portion between point a and c, see Fig. 10. Consequently, the resistivity, ρ = 2.5 × 10^{13} Ω cm and the conductivity (σ = 4 × 10^{-14} S/cm) of the copper sample was determined from Eq. (1).

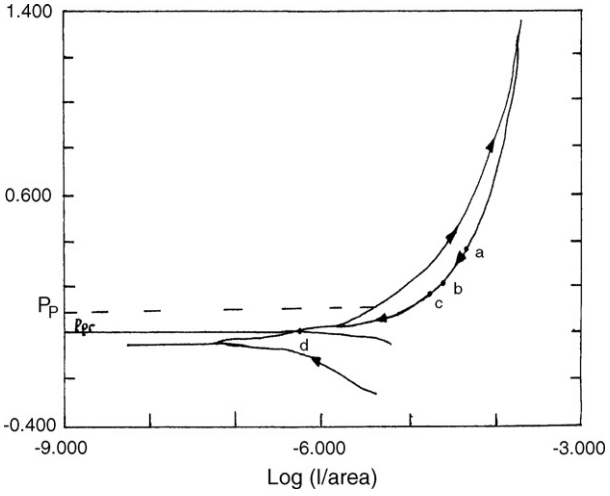

Fig. 9. The cyclic polarization of copper in tap water.

Table 1
Calculated parameters of pure aluminium, UNS No.304 stainless steel, and pure copper in different aqueous solutions.

Sample/solution	Resistance × area(RA) (Ω cm^2)	Total displacement (U) (μm)	Resistivity by OI (ρ) (Ω cm)	Conductivity by OI (σ) (S/cm)	Resistivity by other source [4] (ρ) (Ω cm)
PureAl/seawater	5×10^7	6.52	7.7×10^{10}	1.3×10^{-11}	$2.7\times 10^{-6}5\times 10^{10}$
UNS.304SS/seawater	2.94×10^9	14.84	2×10^{14}	5×10^{-15}	73×10^{-6}
Pure copper/Tap water	8.3×10^9	3.3	2.5×10^{13}	4×10^{-14}	1.7×10^{-6}

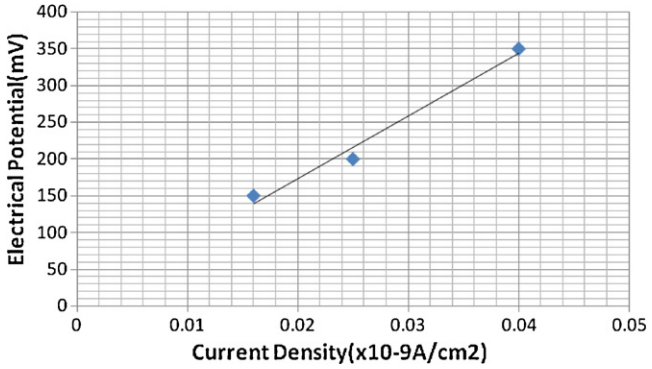

Fig. 10. A plot of the applied electrical potential vs. the corresponding current density, between points a and c in Fig. 9, of the pure copper sample in tap water.

Calculated parameters of resistivity (ρ) and conductivity (σ) of the pure aluminium (in seawater at room temperature), UNS No.304 stainless steel (in seawater at room temperature), and pure copper (in tap water at room temperature) are given in Table 1. Also, electrical resistivity values (ρ) from other source [4] for the pure aluminium (2.7×10^{-6} Ω cm in air at temperature 30 °C), for aluminium oxide, 85% Al_2O_3 (5×10^{10} Ω cm in air at temperature 30 °C), UNS No.304 stainless steel (73×10^{-6} Ω cm in air at temperature 30 °C), and pure copper (1.7×10^{-6} Ω cm in air at temperature 30 °C), are given in Table 1, for comparison sake with the calculated values of this investigation. In addition, there is no measured values for the resistivity of cupric oxide (CuO), cuprous oxide (Cu_2O), or even the oxide of the UNS No.304 stainless steel in literature. It is obvious from Table 1 that the only measured value of the resistivity, in this study, in a good agreement with the one found in literature is for the pure aluminium (7.7×10^{10} Ω cm in seawater at room temperature) and the value of the aluminium oxide, 85% Al_2O_3 (5×10^{10} Ω cm in air at temperature 30 °C). This indicates that holographic interferometry was able to measure the resistivity of oxide films formed on the alloys in this study during the cyclic polarization of the alloys in solutions. Unfortunately, there is no measured value for the resistivity of cupric oxide (CuO), cuprous oxide (Cu_2O), or even the oxide of the UNS No.304 stainless steel in literature comparing those values with the measured values in this study.

References

[1] K. Habib, Measurement of the electrical resistance of aluminium samples in sulphuric acid solutions by optical interferometer techniques, Optik 115 (4) (2004) 145–150.
[2] K. Habib, Model of holographic interferometry of anodic dissolution of metals in aqueous solution, Opt. Lasers Eng. 18 (1993) 115–120.
[3] K. Habib, F. Al Sabti, H. Al-Mazeedi, Optical corrosion-meter, Opt. Lasers Eng. 27 (2) (1997) 227–233.
[4] E. Ray, Bolz, George Tuve (Eds.), CRC of Tables for Applied Engineering and Science, second ed., CRC Press, 1976, pp. 117, 223, 224, 262.